International Journal of Concrete Structures and Materials

RESEARCH Open Access

Bifunctional Multiwall Carbon Nanotubes and Their Effect on Hydration, Conductivity, and Mechanical Properties of Cement Composites

Suthisa Onthong[1,2], Wilasinee Hanpongpun[3], Sakprayut Sinthupinyo[3], Edgar A. O'Rear[4,5] and Thirawudh Pongprayoon[1,2*]

Abstract

Multiwall carbon nanotubes (MWCNTs) significantly enhance hydration reactions and properties of cement composites, expanding their applicability. Interest has grown in the use of multifunctional composites with MWCNTs being a popular filler material to impart additional features. Dispersing MWCNTs in the cement matrix creates an electrical network and replaces pore areas to enhance cement performance. This work compares two novel methods by admicellar polymerization (AP) and grafting polymerization (GP) for preparing bifunctional MWCNTs. Both techniques utilized polyindole (PIn) to enhance electrical conductivity and polyvinyl acetate (PVAc) for better dispersion. Isothermal calorimetry was used to observe the hydration of the cement composites. Results showed that AP-MWCNT/cement and GP-MWCNT/cement increased exothermic heat by 8.4% and 12.1%, respectively, compared to bare MWCNT/cement with the same nanotube content (0.3 wt%). Moreover, both modified MWCNTs improved mechanical properties and electrical conductivity. When comparing AP-MWCNTs and GP-MWCNTs in cement, AP-MWCNT/cement exhibited higher electrical conductivity, while GP-MWCNTs demonstrated superior embedding within the cement matrix, which led to a reduction in pore area and the higher mechanical strength of the two modified MWCNTs.

Keywords Cement hydration, Electrically conductive cement composites, Mechanical strength, Admicellar polymerization, Grafting polymerization, Multiwall carbon nanotubes

1 Introduction

Cement quality and suitability for construction are ensured through tests that assess both its physical and chemical properties. Although traditional cement is valued for its mechanical strength and durability, it struggles to meet the increasing need for sustainability and enhanced functionality in contemporary infrastructure. To overcome the limitations, electricity for multifunctional cement has been combined with the cooperation of structural properties like conductivity, capacitance, and piezoelectricity (Qin et al., 2024). In general, tests of cement evaluate mechanical strength to gauge its ability to withstand loads and, in the case of electrically conductive cement composites (ECCCs), characterization

*Correspondence:
Thirawudh Pongprayoon
thirawudh.p@eng.kmutnb.ac.th
[1] Department of Chemical Engineering, Faculty of Engineering, King Mongkut's University of Technology North Bangkok, Bangkok 10800, Thailand
[2] Center of Eco-Materials and Cleaner Technology, King Mongkut's University of Technology North Bangkok, Bangkok 10800, Thailand
[3] SCG Cement Co., Ltd., Saraburi 18260, Thailand
[4] School of Sustainable Chemical, Biological and Materials Engineering, University of Oklahoma, Norman, OK, USA
[5] Institute for Applied Surfactant Research, University of Oklahoma, Norman, OK, USA

includes observing and measuring electrical conductivity. Recent reports highlight the importance of multifunctional composites such as ECCCs in a wide range of applications including high-speed rail construction (Ding et al., 2022), electrical grounding (J. Zhang et al., 2017), electrical heating (Mohammed et al., 2019), cathodic protection against steel corrosion in concrete (Jing & Wu, 2011) and structural health monitoring (SHM) (Siahkouhi et al., 2021). Additionally, ECCCs are highly sensitive and accurate in detecting the onset of damage from cracking, as well as monitoring both gradual and sudden damage events, ultimately leading, for example, to the complete failure of a maglev girder and demonstrating the significant potential for infrastructure SHM (Ding et al., 2023). ECCCs achieve electrical conductivity through pathways formed when electrically conductive fillers or particles make contact and allow current to flow within the cement matrix (Wang & Aslani, 2019). Conductive nanomaterials such as carbon black, carbon nanofiber, graphene nanoplate, and carbon nanotube (CNT) have gained attention for developing ECCCs, yet CNTs stand out due to their distinctive structure and notable features, including a high aspect ratio, electrical conductivity and an enhanced reinforcement effect in cement composites (Wang & Aslani, 2019). How multiwall carbon nanotubes (MWCNTs) affect hydration and these reactions is an important question to understanding the relationship between filler and composite strength.

The evolution of mechanical properties in cement-based materials is closely tied to the hydration reactions between cement and water (He et al., 2023; Pang et al., 2021). Reaction conditions are crucial in cement technology for mix optimization and predicting structural performance. To understand the transformation during cement hydration, heat evolution is normally observed and divided into five distinct zones, as shown in Fig. 1 (Vazquez & Pique, 2016). In the initial stage (shortly after mixing), tricalcium aluminate reacts with water to form an aluminate-rich gel and then combines with sulfate to generate ettringite crystals (Preece et al., 2001; Yuenyongsuwan et al., 2019). A few minutes later, a low heat evolution can be observed during the dormant or induction period, when tricalcium silicate and dicalcium silicate in the cement begin to react and form a gel of hydrated calcium silicate and portlandite. This phase significantly contributes to develop the strength of cement (Marchon & Flatt, 2016; Scrivener et al., 2019). After that for several hours, the early-formed ettringite transforms into monosulfoaluminate and allows the hydration process of tricalcium aluminate within the cement paste. Lastly, tetracalcium aluminoferrite undergoes a similar reaction to the aluminate, but at a slower pace (Aïtcin, 2016; Copeland et al., 1960).

Many researchers have reported nucleation enhancement and acceleration of cement hydration as the high surface area of MWCNTs increases available reaction sites (MacLeod et al., 2021; Mendoza et al., 2014). Their use generates high crystallinity of hydration products with densification yielding increased strength of cement composites. However, MWCNTs have a tendency to form bundles, wherein numerous tubes are interconnected through van der Waals forces. To avoid the presence of agglomerates, researchers need to modify the MWCNTs

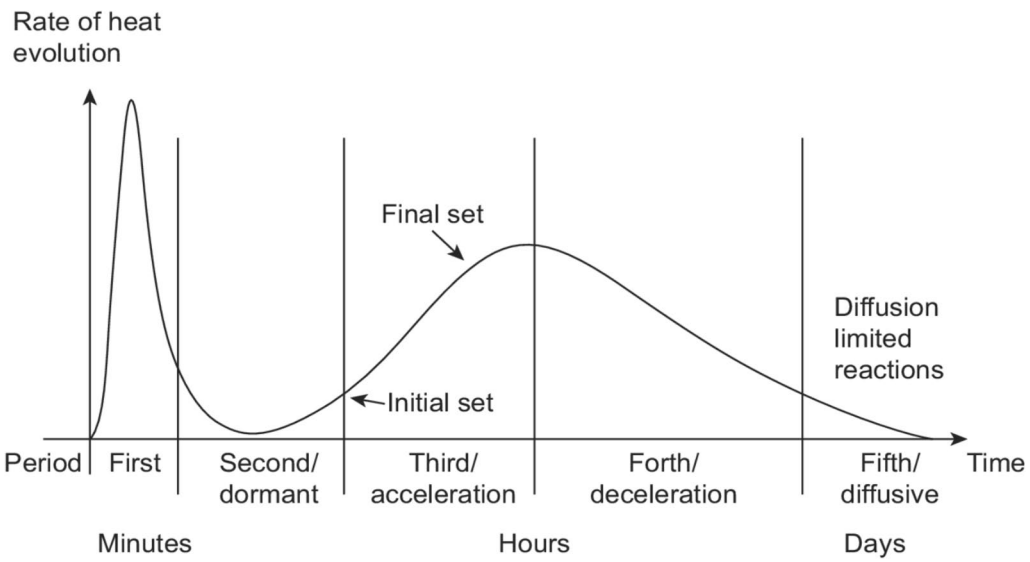

Fig. 1 Stages of cement exothermic reaction (Vazquez & Pique, 2016)

so that good dispersion occurs during preparation for cement hydration. Numerous methods have been used to disperse MWCNTs for cement work including mechanical techniques (e.g., ultrasonication, ball-milling, plasma treatment) and surface modification techniques (adding surfactants or enhancing hydrophilicity through chemical functionalization). MWCNTs are frequently used without and with the chemical functionalization for cement (O'Rear et al., 2023). The functionalization allows the combination of nanotube with substituent materials like water-soluble and electrical polymers, typically categorized as either non-covalent or covalent forms in relation to bonding between MWCNTs and the functionalizing species. The modification on the surface of particles enhances the dispersion and other specific properties of materials. Admicellar polymerization (AP) and grafting polymerization (GP) are the most interesting techniques to implement world-wide application including construction. AP is simple and scalable, improving dispersion and interface bonding without altering the particle structure of non-covalent linking (Hanumansetty et al., 2015). In contrast, GP forms covalent bonds between polymer chains on the particle surface, improving charge transfer and enhancing integration into the material matrix for a more durable modification due to the stronger covalent bonds (Li et al., 2022). Both AP and GP modification of MWCNTs have limited research comparing between the two methods, applied in the cement.

This work studied the effect of MWCNTs without and with functionalization on cement hydration, resulting in better strength and conductivity for application as ECCCs. The cement hydration was observed from heat evolution by isothermal calorimetry, calcium silicate hydrate (C-S–H) formation by XRD, and porosity inside cement matrix by analysis of SEM images with ImageJ software. The flexural and compressive strengths of the cement composites were measured following ASTM C348 and ASTM C109. Importantly, the electrical conductivity of the cement composites was tested using an electrometer/high resistance according to ASTM D-257 standard.

2 Materials and methods

2.1 Materials

Multiwalled carbon nanotubes (MWCNTs) obtained from Nano Generation Co., Ltd (Thailand) were modified through concurrent admicellar polymerization (AP-MWCNTs) and grafting-from polymerization (GP-MWCNTs) according to our previous reports (Onthong et al., 2022) and (Onthong et al., 2023), respectively. AP-MWCNTs and GP-MWCNTs were prepared under optimal conditions with a consistent 0.4:1 ratio between indole (In) and vinyl acetate (VAc) monomer. Table 1 presents the physical properties of both bare and modified MWCNTs in the relation of cement application. Portland cement type I was procured from SCG Cement Co., Ltd (Thailand).

2.2 Preparation of cement pastes and cement composites

The formulation of cement pastes and cement composite samples is presented in Table 2 for observing the effect of bare and modified MWCNTs. The cement was mixed with a fixed water-to-cement ratio of 0.36 (Amziane, 2006), following ASTM C305 standard.

2.2.1 Cement Hydration Reaction by Isothermal Calorimeter

The calorimetry tests of cement were performed according to ASTM C1702-17 using an eight-channel calorimeter (TAM Air 8 channel, TA Instrument, USA) equipped with a thermostat that maintains temperature stability at ± 0.02 °C and has a precision of ± 2 μW (± 0.07% heat evolution) with an accuracy of greater than 95%. Hydration rate was assessed at 1-min intervals as power (W) and normalized per weight (g) of cement. The water–cement ratio (w/c) for the mixture was 0.36. Water (14.4 g) and a specified percentage (Table 2) of the

Table 1 Physical properties of MWCNTs and modified MWCNTs

Physical properties	Nanomaterials		
	MWCNTs	AP-MWCNTs (Onthong et al., 2022)	GP-MWCNTs (Onthong et al., 2023)
Diameter (nm)	11.43	17.82	27.55
Functional group	–	-C = O, -NH	-C = O, -NH
Spreading coefficient (mN/m)	− 118.6	− 59.03	-50.4
Electrical conductivity (S/cm)	5.34×10^4	6.98×10^2	5.48×10^2

The diameters were determined through ImageJ software analysis of the FESEM images. A normal probability distribution was generated from 25 measurements using Minitab software. FTIR analysis (INVENIO-S, Bruker, United Kingdom) was employed to identify the functional groups. Hydrophobicity (water spreading) was assessed using a contact angle device (OCA 15LJ, DataPhysics Instruments, Germany), while electrical conductivity was measured with an Electrometer/High Resistance Meter (Keithley, Tektronix, United States)

Table 2 Mix proportions of cement composites for investigation

Specimens	OPC (g)	Water (g)	Nanoparticle (g)		
			MWCNTs	AP-MWCNTs	GP-MWCNTs
Cement	1000	360	–	–	–
0.05MWCNT/C	1000	360	0.5 *	–	–
0.3MWCNT/C	1000	360	3		
0.7MWCNT/C	1000	360	7	–	–
0.3AP-MWCNT/C	1000	360	–	3	–
0.3GP-MWCNT/C	1000	360	–	–	3

* 0.05 wt% MWCNTs demonstrate good mechanical strength (Onthong et al., 2022, 2023)

studied MWCNTs were mixed with cement (40 g) using a high-speed mixer (Ika Eurostar 20 digital, 1600 rpm) for 2 min in a testing cup. The prepared specimen was then carefully weighed (5 g) and transferred to a testing glass bottle, which was placed in the calorimeter. The measurements were taken over a 70-h observation period (Yuenyongsuwan et al., 2019).

2.2.2 Crystallinity of minerals in cement by XRD characterization

The crystalline structure of chemical components in cement was determined using XRD at different curing periods of 7, 14, and 28 days. The cement specimens were ground and sieved by a 75-mm IS sieve and then subjected for mineralogical composition analysis. XRD patterns of the grounded cement samples were obtained from the SmartLab X-Pert Pro Diffractometer (Rigaku, USA) with Cu Kα radiation (λ = 1.541 Å, 40 kV/100 mA) at a deflection angle ranging from 10° to 80° and at a scanning speed of 5°/min.

2.2.3 Structural morphology of cement composites by SEM

The microstructure development over time in cement composites was analyzed by SEM (JEOL JSM-IT500HR, JEOL, Japan). The cement specimens were fabricated according to the ratios specified in Table 2 and subjected to curing at room temperature with different durations of 7, 14, and 28 days. Samples were sputter coated with a thin layer of gold before capturing the images using SEM. ImageJ software was used to analyze the porosity of cement composites with SEM images magnified at 25,000x (AlMarzooqi et al., 2016; Saghiri et al., 2017).

2.2.4 Mechanical strength

The impact of concentration of the MWCNTs on the flexural and compression properties of the cement composites was studied though mechanical analysis. Prismatic beam specimens of dimensions 40 × 40 × 160 mm^3 and cubic specimens of 50 × 50 × 50 mm^3 were used to measure the flexural and compressive strengths, respectively. The flexural test (three-point bending) was performed according to ASTM C348 by a flexural testing machine (NL 4008 X/003 & 004, NL scientific, Malaysia) at a loading rate of 0.04 kN/s. The compressive test was carried out according to ASTM C109 by a universal testing machine (STS-C092V, SOIL TESTING SIAM, Thailand) with a loading rate of 1.80 kN/s. Five specimens were tested to check the repeatability of the results.

2.2.5 Electrical conductivity

Electrical conductivity of the cement composites was tested using an electrometer/high resistance meter (Keithley, Tektronix, USA), with a stainless-steel plate utilized as an electrode, following the ASTM D-257 standard from five individual specimens. The dimensions of the specimen are 80-mm diameter and 6-mm thickness. The electrical conductivity was calculated from the measured electrical resistance (R_v) based on Eq. (1):

$$\sigma = \frac{t}{R_v \times A}. \tag{1}$$

σ represents the electrical conductivity (S/cm), t stands for the average thickness of the cement paste pellet (cm), R_v represents the electrical resistance (Ω), and A denotes the capacitive displacement area of the guarded electrode (cm^2) (Onthong et al., 2022).

3 Results and discussion

3.1 Cement hydration without/with MWCNTs

To investigate cement hydration behavior, isothermal calorimetry measures the heat flow during cement paste hydration. Figure 2a shows the exothermic curves of cement hydration for samples with bare MWCNTs added across a range of 0.05–0.7 wt%. It was observed that the MWCNTs reduce the time to reach the main exothermic peak from 9.07 min in plain cement paste to 8.12, 8.03, and 8.29 min on adding 0.05, 0.3, and 0.7 wt% MWCNTs, respectively, indicating faster initial hydration reactions

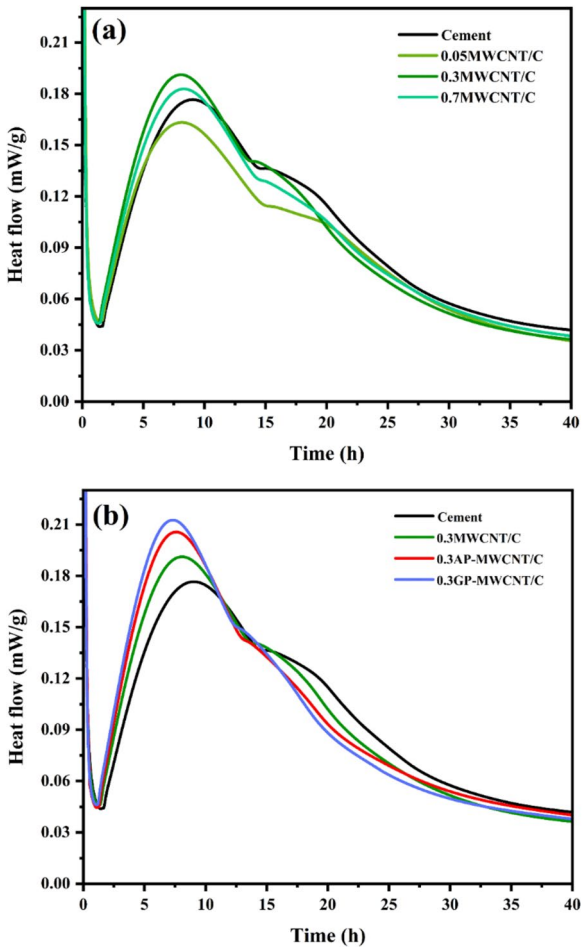

Fig. 2 Hydration behavior of cement composites for comparison between: **a** MWCNTs content and **b** different MWCNTs at 0.3 wt%

than the plain cement paste control sample. This acceleration is attributed to the nucleation effect of MWCNTs, which facilitates the rapid formation of nuclei in the cement component, promoting the occurrence of the hydration reaction (Xiaonan Wang et al., 2022a, 2022b). At low concentration of MWCNTs, hydrophobic nanotubes associated with the paste inhibit water migration and drive water into pores, working against hydration. At higher MWCNTs concentrations, hydrophobic agglomerates form and fill the larger pores, reducing their ability to retain water and reduce hydration. From the results, cement by adding 0.05 wt% MWCNTs released 7.9% less heat than that released by the cement paste, while adding 0.7 wt% MWCNTs in cement released 3.4% more heat than that of cement, but 0.7% lower than the heat from adding 0.3 wt% MWCNTs to the cement. This finding indicated that 0.3 wt% MWCNTs could be the optimum according to greater distribution during hydration and not so much as to cause aggregation disrupting hydration (Liu et al., 2003). Therefore, MWCNTs at a dosage of 0.3 wt% were selected for further investigation, using different MWCNTs to study the effect of chemical functionalization on the properties of cement composites.

Figure 2b illustrates the effects of different MWCNTs at a dosage of 0.3 wt% on the cement hydration process. It was observed that the time to reach maximum for both AP-MWCNT/C and GP-MWCNT/C was 7.57 and 7.19 min, respectively, faster than that of bare MWCNT/C. Moreover, the highest exothermic heat of AP-MWCNT/C and GP-MWCNT/C increased by 8.4% and 12.1%, respectively, compared to bare MWCNT/C. This improvement can be explained by the presence of carbonyl groups (C=O) in the PVAc chain, which enhance the dispersion and interaction of MWCNTs with the cement matrix (Onthong et al., 2022; Vaičiukyniene et al., 2012). Hydrophilic groups facilitate migration of water along the nanotube and into the paste to improve hydration. Furthermore, when comparing the effects of AP-MWCNTs and GP-MWCNTs on the exothermic heat from the hydration reaction of cement composites, GP-MWCNTs exhibited a higher exothermic heat than AP-MWCNTs, despite using the same polymer type and content (e.g., polyindole (PIn) and polyvinyl acetate (PVAc)). With the different bonding of physical interaction of AP method and chemical interaction by covalent bond of GP method, GP-MWCNTs enhanced greater dispersion, confirmed by SEM images in Fig. 5, promoting the cement hydration at the interfacial transition zone (ITZ) of increasing the number of nucleation sites within the interfacial microstructures of the cement matrix through nanotubes (Han et al., 2017; Xinyue Wang et al., 2022a, 2022b). In contrast, AP-MWCNTs result in only physically adsorbed polymer layers and involve the use of surfactants, which might create bubbles and lead to increased porosity within the cement matrix, thereby resulting in weaker interactions with the C-S–H products (Xinyue Wang et al., 2020). This effect was confirmed by the strength of cement for comparison in Table 5.

3.2 Calcium silicate formation from cement hydration without/with MWCNTs

XRD analysis was performed to investigate the crystallization of the components in the cement materials after curing. Figure 3 presents the XRD patterns of the hydrated cement of four samples containing cement (Fig. 3a) and cement composites with 0.3 wt% of MWCNTs (Fig. 3b), AP-MWCNTs (Fig. 3c), and GP-MWCNTs (Fig. 3d) at various curing times of 7, 14, and 28 days. The presence of calcium hydroxide (CH) is confirmed by diffraction peaks at $2\theta = 34.06°$ and 47.05° (PDF 00-001-1079 (Hanawalt et al., 1938)). Additionally, peaks at $2\theta = 23.18°$, 29.46°, 32.07°, 32.72°, 35.92°, 39.42°, and 43.17° indicate the presence of C-S–H tobermorite-like crystals (PDF

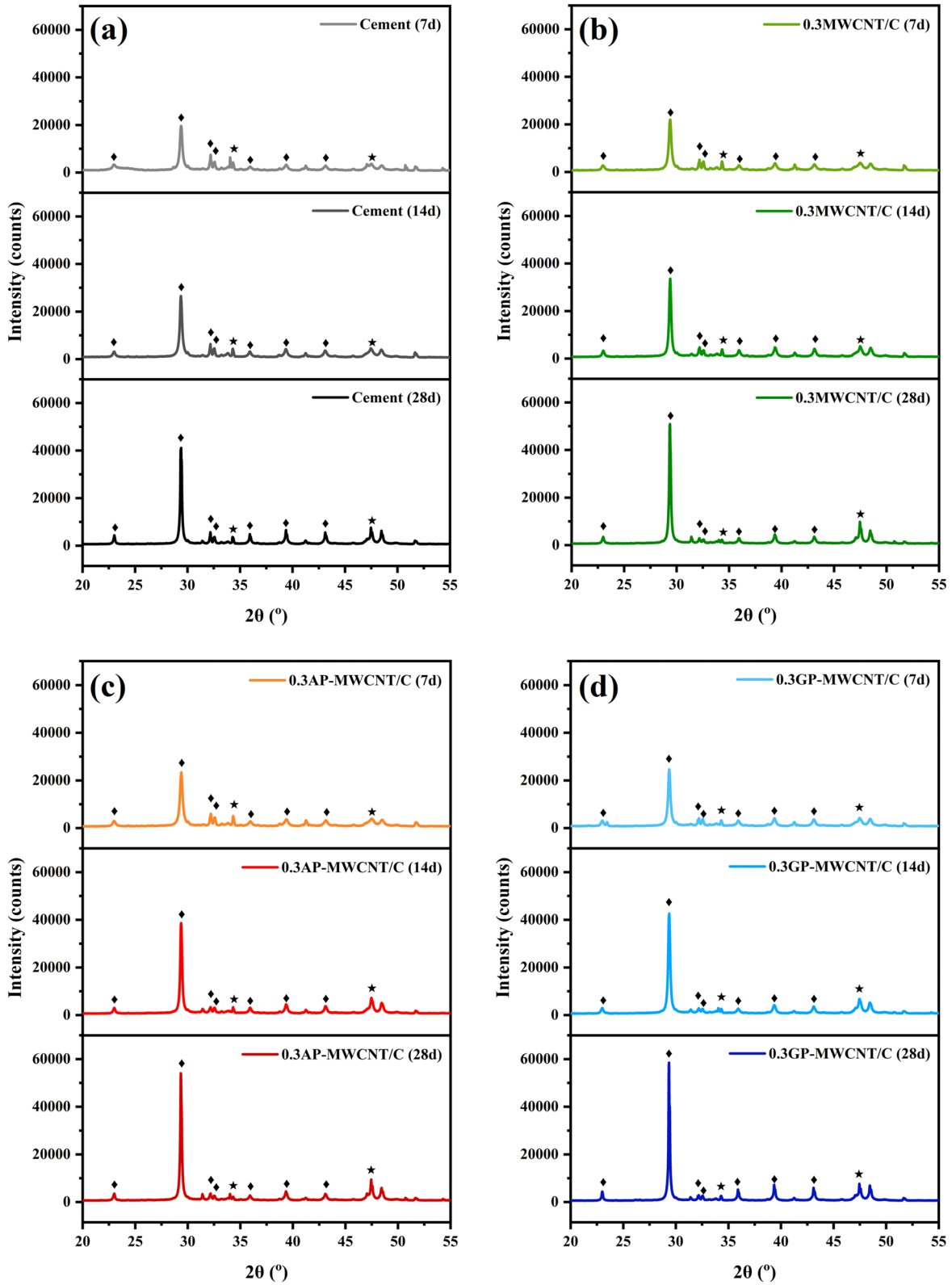

Fig. 3 XRD patterns of cement sample at different curing ages of: **a** cement, **b** 0.3MWCNT/C, **c** 0.3AP-MWCNT/C, and **d** 0.3GP-MWCNT/C (♦: C-S–H and ★: CH)

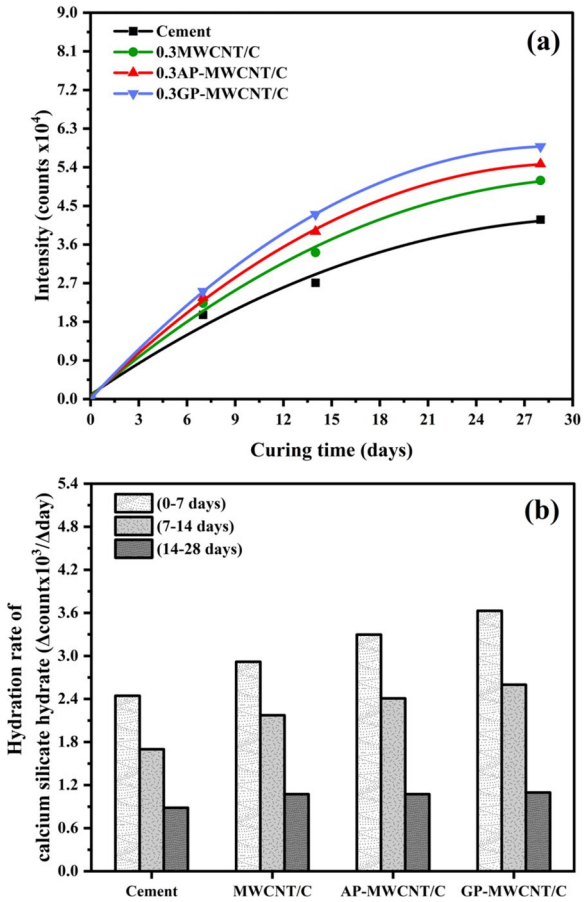

Fig. 4 **a** C-S–H intensity (at 2θ = 29.46°) formed in cement matrix at various curing ages and **b** rate of C-S–H growth at three curing periods of 0–7, 7–14 and 14–28 days. Curves shown are quadratic fits using polynomial regression.

01-083-1520 (Hamid, 1981)). Notably, no new diffraction peaks were observed in the cement composites compared to the cement control sample, suggesting that the incorporation of MWCNTs or PIn/PVAc modified MWCNTs (prepared by AP and GP methods) do not lead to the formation of new phases (Cui et al., 2017). However, XRD results show a significant difference in intensity at 2θ = 29.46° for C-S–H, indicating variations in nanoadditives and curing time. This confirms that both variations influenced the degree of C-S–H formation in the cement matrix.

The intensity of C-S–H at 2θ = 29.46° with various curing times of cement and MWCNTs/cement composites in Fig. 4a was observed for studying the rate of cement hydration as shown in Fig. 4b for three curing periods of 0–7, 7–14 and 14–28 days. The rate of hydration in various periods was estimated from the slope of the curves of each period. It was found that the crystallinity peak of C-S–H rose with curing time, whereas the rate of hydration was slowed down. For plain cement paste, during the second period (7–14 days), the rate of hydration decreased by 30.6% compared to the previous period (0–7 days). Furthermore, in the third period (14–28 days), the rate declined further by approximately 48.2% relative to the second period. When MWCNTs or modified MWCNTs were added, a similar behavior was observed, with the rate of hydration decreasing in the same manner as in the plain cement paste. This is because the early stages in the cement matrix have a high reaction between surface area of cement powder and water for transforming calcium and silicate ions to be C-S–H hardened cement (Bullard et al., 2011). Then, the hydration rate slows down due to a denser of C-S–H hardened cement, impeding the diffusion of water molecules for continuous hydration reaction (Scrivener et al., 2019).

The modified MWCNTs exhibit the fastest rate compared to the unmodified MWCNTs and control samples due to better dispersion, which enhances the contact pattern and accelerates the hydration reaction (Torabian Isfahani et al., 2016). A two-way ANOVA statistical method was used to investigate the impact of different methods for modifying MWCNTs (AP-MWCNTs and GP-MWCNTs) and curing ages (7, 14, and 28 days) on the rate of C-S–H formation, as presented in Table 3. F-ratio represents the ratio of the mean square (MS) between groups to the MS within the samples of each group and F-critical is the threshold value of the F-statistic at a significance level (α) of 0.05, representing the

Table 3 Statistical analysis of hydration rate of calcium silicate hydrate by ANOVA: two-factor analysis of the types of modified MWCNTs and curing ages

Source of variation	SS[1]	df[2]	MS[3]	F-ratio	F-critical	p-value
Hydration rate of calcium silicate hydrate (Δcount × 10^3/Δday)						
Types modified MWCNTs*	0.050	1	0.050	4.169	18.513	0.1779
Age of samples **	5.723	2	2.861	240.996	19.000	0.0041
Error	0.024	2	0.012			
Total	5.796	5				

SS[1]: sum of squares, *df*[2] degrees of freedom, *MS*[3] mean square

Types modified MWCNTs* are the two different methods for modified MWCNTs including AP-MWCNTs and GP-MWCNTs

Age of samples** refers to the varying age of cement samples during different curing times at 7, 14, and 28 days

Cement composites by adding 0.3 wt% of AP-MWCNTs or GP-MWCNTs

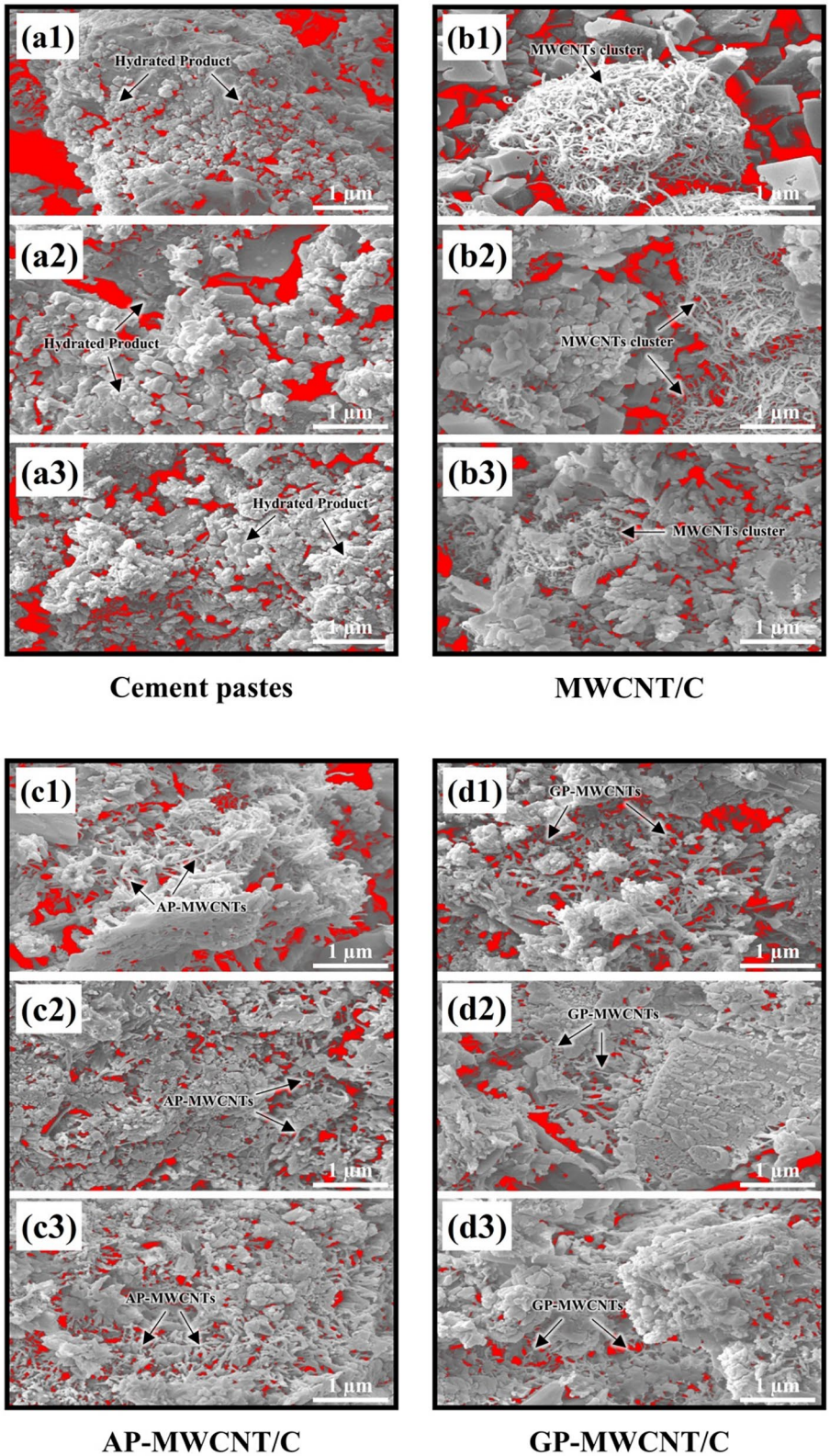

Fig. 5 SEM micrographs with porosity using ImageJ analysis (red) at 25,000 × of cement at three curing ages of 7, 14 and 28 days for comparison of: **a** cement, **b** 0.3MWCNT/C, **c** 0.3AP-MWCNT/C, and **d** 0.3GP-MWCNT/C

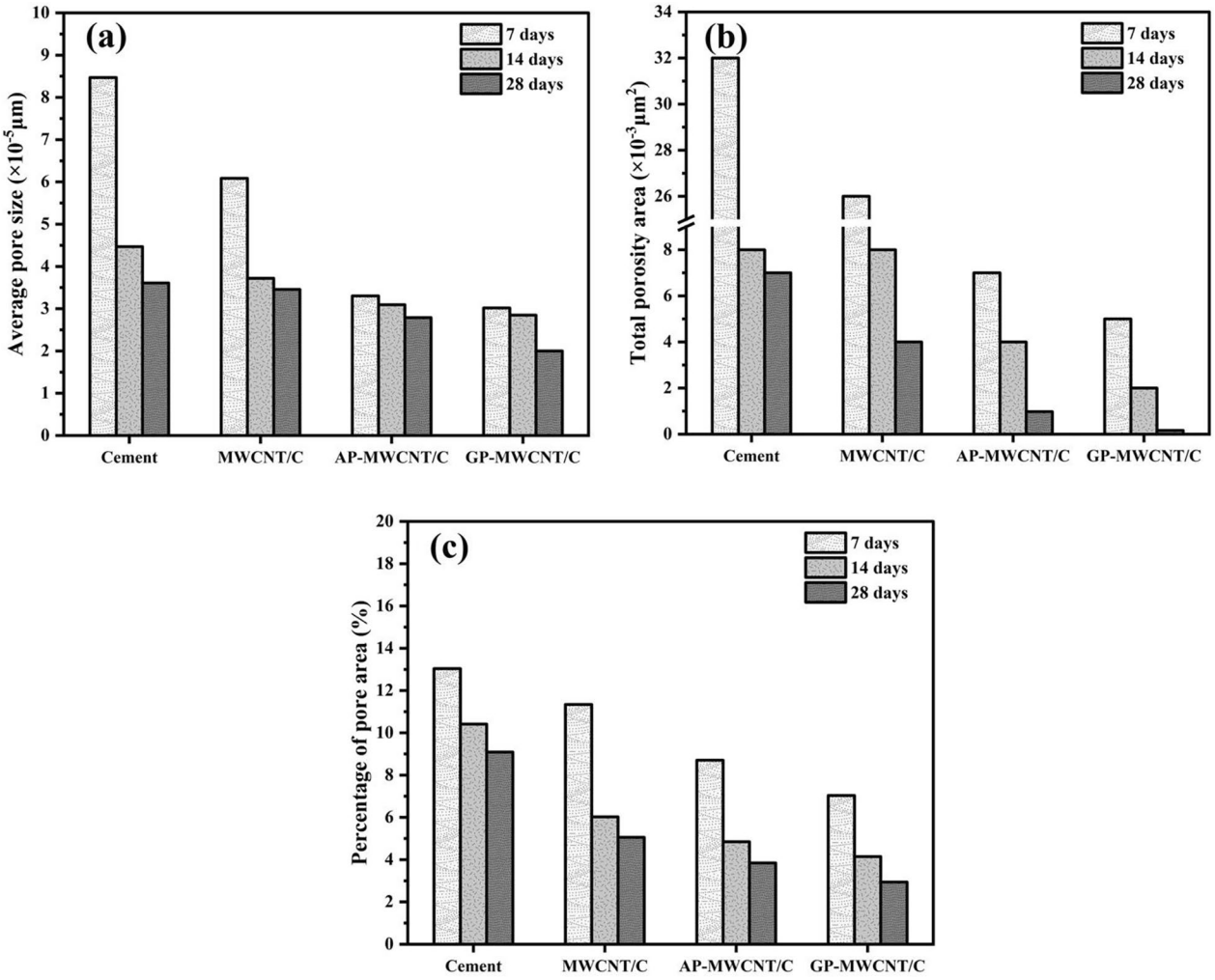

Fig. 6 Numerical data analyzed by ImageJ from SEM micrographs of (**a**) average pore size, **b** total porosity area and **c** percentage of pore area of cement without/ with different MWCNTs of 0.3 wt% at various curing ages

probability of mistakenly rejecting a true null hypothesis (H_0). If the F-ratio is greater than F-critical, there is sufficient evidence to reject H_0, indicating that at least one group of the investigated factor differs from the others (Vinod et al., 2019; Wahid et al., 2018). The results indicate that the F-ratio for the age of the sample surpassed the F-critical value, and the p-value was also lower than 0.05, indicating that the curing age was significant for C-S–H formation (Dowdy et al., 2011; Ståhle & Wold, 1989). In contrast, the difference in adding AP- and GP-MWCNTs to cement composites did not present a significant difference in hydration rate and C-S–H formation, as indicated by a lower F-ratio compared to the F-critical value and a p-value higher than 0.05, possibly due to both having good dispersion in the cement matrix (Onthong et al., 2022, 2023).

3.3 Microstructure and porosity area analysis in cement pastes without/with MWCNTs

The microstructure and porosity within the cement matrix were investigated using SEM, as shown in Figs. 5 and 6**.** Imaging indicated MWCNTs dispersion and pore structure and offered insights into the integration of MWCNTs into the samples. Figure 5 shows that the bare MWCNTs agglomerate in the cement matrix, whereas the modified MWCNTs contribute to better dispersion in the cement matrix. Improving the dispersion of the nanofillers is crucial for enhancing the mechanical and electrical properties of the cement composite, as well as promoting better interfacial bonding and mechanical strength (Páez-Pavón et al., 2022; Sun et al., 2016; Zhang et al., 2023).

The average pore size, total porosity area and percentage of pore area within the cement sample in Fig. 6

Table 4 Statistical analysis of average pore size, total porosity area and percentage of pore area in cement by ANOVA: two-factor analysis of the types of modified MWCNTs and curing ages

Source of variation	SS[1]	df[2]	MS[3]	F-ratio	F-critical	p-value
Average pore size ($\times 10^{-3}$ μm)						
Types modified MWCNTs*	0.292	1	0.292	6.398	18.513	0.1270
Age of samples**	0.6362	2	0.318	6.975	19.000	0.1250
Error	0.0912	2	0.046			
Total	1.019	5				
Total porosity area ($\times 10^{-3}$ μm^2)						
Types modified MWCNTs*	3.866	1	3.866	16.545	18.513	0.0554
Age of samples**	29.614	2	14.807	63.375	19.000	0.0155
Error	0.467	2	0.234			
Total	33.947	5				
Percentage of pore area (%)						
Types modified MWCNTs*	2.133	1	2.135	22.177	18.513	0.0423
Age of samples**	24.241	2	12.121	126.051	19.000	0.0078
Error	0.192	2	0.096			
Total	26.566	5				

SS[1]: sum of squares, *df*[2] degrees of freedom, *MS*[3] mean square

Types modified MWCNTs* are the two different methods for modified MWCNTs including AP-MWCNTs and GP-MWCNTs

Age of samples** refers to the varying age of cement samples during different curing times at 7, 14, and 28 days

Cement composites by adding 0.3 wt% of AP-MWCNTs or GP-MWCNTs

indicate that with increasing curing time, the pore area within the cement sample decreases, in accord with the increase of C-S–H hydrate products (Neves Junior et al., 2015; Zhao et al., 2018). Furthermore, the curing age at 14 and 28 days presents a slight change of pore area. Compared with bare MWCNTs, the modified MWCNTs provided more effective connection bridges to fill the porous gaps and embed in hydrated cement. The impacts of modified MWCNTs and curing age on the pore space within the cement matrix were investigated using two-factor ANOVA statistical analysis, as depicted in Table 4. The results show that the F-ratio for both modified MWCNTs and sample age was lower than the F-critical value. Moreover, the p-values for both parameters were greater than 0.05, indicating that neither the modification methods nor the curing age had a statistically significant effect on the average pore size in the cement composites. In terms of total porosity area, the F-ratio for modified MWCNTs was lower than the F-critical value (p-value > 0.05), while the F-ratio for sample age exceeded the F-critical value (p-value < 0.05), providing sufficient evidence that sample age significantly affected the total porosity area, whereas the modification methods did not. Regarding the percentage of pore area, the F-ratios for both modified MWCNTs and sample age exceeded the F-critical value, and the p-values for both were less than 0.05, indicating that both parameters significantly influenced the percentage of pore area in the cement composites. This is due to the difference in spreading coefficient which reflects surface properties of AP-MWCNTs and GP-MWCNTs. GP-MWCNTs had a lower spreading coefficient (less negative) and were much closer to the cement matrix than the AP-MWCNTs, resulting in a lower percentage of pore area of GP-MWCNT/C than AP-MWCNT/C (O'Rear et al., 2023). Sequential admicellar polymerization produced an even lower spreading coefficient (− 45 mN/m), but its effect on pore structure has not been found (Onthong et al., 2024). However, the two-factor ANOVA analysis of the average pore size and total porosity area suggests that the modification method of the MWCNTs did not have a significant effect, nor did the curing age influence the average pore size. Future tests, particularly those assessing the properties showed in Fig. 7, are needed to further validate these findings.

3.4 Mechanical strength and electrical conductivity

The mechanical strength and electrical conductivity of cement composites were examined at different curing times to confirm the impact of the studied MWCNTs. The cement paste without any additives of MWCNTs was used as the control sample. The flexural and compressive strengths were measured of all samples with the results in Fig. 7a and b, respectively. When increasing the curing time, the strengths increased sharply in the early period and then less so in line with a slower

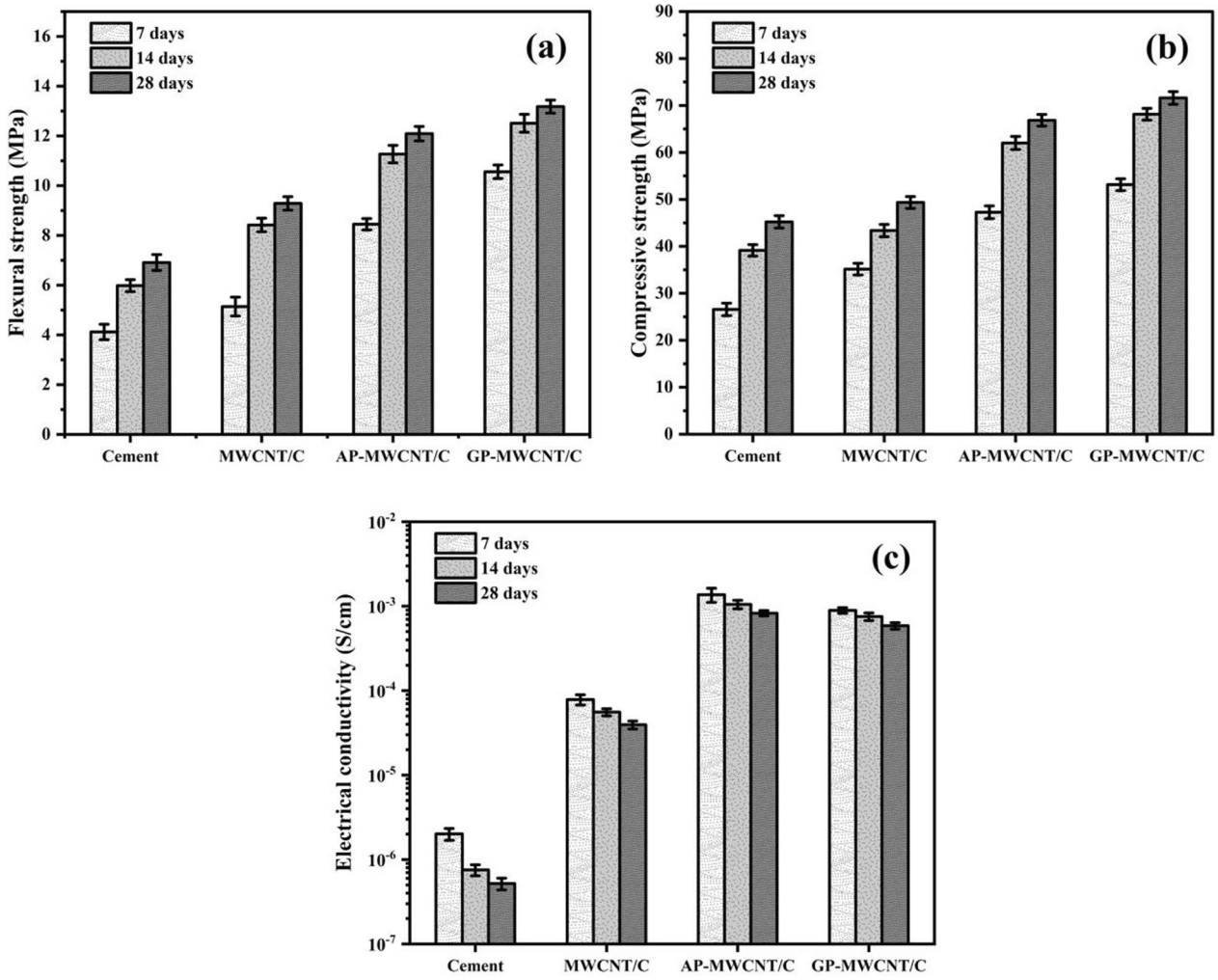

Fig. 7 a Flexural strength, b compressive strength and c electrical conductivity of cement without/ with different MWCNTs of 0.3 wt% at various curing ages

rate of formation of C-S–H hydration products. Conversely, the electrical conductivity of cement composites decreased with time as Fig. 7c due to hindered ion mobility with the increase of C-S–H hydration products acting as insulators in the materials. Han et al. (Han et al., 2015) reported that, in cement mortar (with sand), the control sample and those containing CNT/carbon black composite fillers ranging from approximately 0.75–5.96 wt% show a decrease in electrical conductivity with curing age from 1 to 3 days, stabilizing after 3 days. After the standard 28-day curing period, flexural strength of the 0.3 wt% MWCNT sample at 9.29 MPa was comparable to a value of 9 MPa from the literature while compressive strength at 49.35 MPa was notably higher than a reference result of 24 MPa (O'Rear et al., 2023). The observed electrical conductivity of 3.94×10^{-5} S/cm in this study was the same order of magnitude as previously reported (Dong et al., 2019). Compared to Sun et al.'s (Sun et al., 2017) study, cement composites filled with nano-graphite platelets (approximately 2.27 wt%) for 28 curing days exhibited no piezoresistive effect. In this study, cement composites incorporating modified MWCNTs at the same loading (0.3 wt%) exhibited greater improvements in mechanical and electrical properties compared to those with bare MWCNTs. After 28 days of curing, the AP-MWCNT/C exhibited a flexural strength of 12.09 MPa, compressive strength of 66.85 MPa, and electrical conductivity of 8.27×10^{-4} S/cm while GP-MWCNT/C demonstrated a flexural strength of 13.18 MPa, compressive strength of 71.59 MPa, and electrical conductivity of 5.86×10^{-4} S/cm. Results confirm that the modified MWCNTs enhanced the mechanical properties and electrical conductivity of the cement composites better than the bare MWCNTs. Comparing these findings with existing literature reveals both consistencies and variations. Cheng et al. (Cheng et al., 2023)

Table 5 Statistical analysis of flexural strength, compressive strength, and electrical conductivity of cement composites by ANOVA: two-factor analysis of the types of modified MWCNTs and curing ages

Source of variation	SS[1]	df[2]	MS[3]	F-ratio	F-critical	p-value
Flexural strength (MPa)						
Types modified MWCNTs*	18.802	1	18.802	77.426	4.600	< 0.0001
Age of samples**	59.982	14	4.284	17.643	2.484	< 0.0001
Error	3.399	14	0.243			
Total	82.184	29				
Compressive strength (MPa)						
Types modified MWCNTs*	200.105	1	200.105	203.798	4.600	< 0.0001
Age of samples**	1859.716	14	132.837	135.289	2.484	< 0.0001
Error	13.746	14	0.982			
Total	2073.568	29				
Electrical conductivity (S/cm)						
Types modified MWCNTs*	7.626×10^{-7}	1	7.627×10^{-7}	163.022	4.600	< 0.0001
Age of samples**	8.432×10^{-7}	14	6.023×10^{-8}	12.876	2.484	< 0.0001
Error	6.549×10^{-8}	14	4.678×10^{-9}			
Total	1.671×10^{-6}	29				

SS[1] sum of squares, *df*[2] degrees of freedom, *MS*[3] mean square

Types modified MWCNTs* are the two different methods for modified MWCNTs including AP-MWCNTs and GP-MWCNTs

Age of samples** refers to the varying age of cement samples during different curing times at 7, 14, and 28 days

Cement composites by adding 0.3 wt% of AP-MWCNTs or GP-MWCNTs

investigated the effect of MWCNTs size on the electrical properties of cement mortar, finding that MWCNTs with diameters of 10–20 nm at 0.1 wt% exhibited better conductivity than those with larger diameters. In addition, a 0.75 wt% MWCNTs loading produced the most significant fractional change in resistivity, indicating enhanced piezoresistive behavior. Chen and Li (2024) reported that incorporating 0.1% MWCNTs with 5% silica fume achieved a maximum compressive strength of 116.5 MPa, which was 12% greater than that of plain cement paste. When 0.1% MWCNTs and 10% silica fume were added, flexural strength increased to 11.5 MPa, and the loss factor improved by up to 22.59%. Similarly, Cerro-Prada et al. (2021) found that a 0.02 wt% MWCNTs loading led to a 25% and 20% increase in compressive and flexural strengths, respectively, after 90 days. Mortars containing 0.01–0.015 wt% MWCNTs also showed a reduction in resistivity by up to 10% at both 28 and 90 days.

When comparing the addition of AP-MWCNTs and GP-MWCNTs to cement pastes, it was found that the electrical conductivity of AP-MWCNT/C was higher than that of GP-MWCNT/C, while the mechanical strength was lower. The conformational structure of the polymers and the interaction between the polymers and MWCNTs from AP method and GP method and cement matrix present the different mechanisms. The former one, AP-MWCNTs are formed on the polymeric surface with physical interaction of the surfactant layer, binding between MWCNTs surface and polymer film, whereas GP-MWCNTs are linked by chemical interaction with covalent bond between MWCNTs surface and polymer film. For enhanced conductivity of AP-MWCNTs, Genetti et al. proposed that conducting polymers formed by AP lead to molecular wires with entanglements above the percolation threshold to facilitate electron transfer (Genetti et al., 1998). The surfactant in AP method may also lead to a greater increase in conductivity due to its ionic molecule, using sodium dodecyl sulfate (SDS), which tend to localize the polymerization closer to greater contact at the surface between the PIn, as an electrically conductive polymer, and MWCNTs. This reason assists in a more uniform and intimate PIn formation on the MWCNTs surface (Hanumansetty et al., 2015; Rauniyar & Bhattarai, 2021). In contrast, the mechanical properties of GP-MWCNT/C were superior, as the GP technique creates stronger covalent bonds between the grafted polymer and MWCNTs, improving interfacial interaction with cement more effectively than those of AP-MWCNTs (Basheer et al., 2020; Sun et al., 2016). Moreover, the residual surfactant from the AP process may have led to bubble formation inside the cement matrix, affecting porosity and limiting the increase in mechanical strength (Metaxa et al., 2022).

Table 5 presents a two-factor ANOVA analysis of the two different modified MWCNTs and the properties at three curing ages. It was significant due to using

different modified MWCNTs and curing age indicated by an F-ratio higher than F-critical and a p-value < 0.0001 which is less than 0.05. Practically, these results suggest strong potential for advanced construction materials. From these results, GP-MWCNT/C and AP-MWCNT/C can be applied in structural elements requiring high strength and superior conductivity, which would be will-suited for smart functional works like self-sensing concrete or de-icing pavements. Moreover, the long-term stability of these properties supports their viability in real infrastructure. Nonetheless, further evaluation of scalability, cost, and environmental impact is essential before widespread implementation.

4 Conclusion

The modified MWCNTs by AP and GP enhanced cement hydration, indicated by increased heat release and a faster time to reach the main exothermic peak, with the optimum quantity at 0.3 wt%. The results indicated that AP-MWCNT/C and GP-MWCNT/C enhance exothermic heat by 8.4% and 12.1%, respectively, when compared to bare MWCNT/C. The greater release of heat with GP-MWCNTs occurs even though the same polymer type of PIn and PVAc were present. GP-MWCNTs enhanced the dispersion and accelerated hydration of cement at the ITZ more than the AP-MWCNTs did. The cement composite with the graft polymer nanotubes exhibited greater mechanical strength as a result of the covalent bond interaction. AP-MWCNTs had smaller increases in mechanical strength with weaker physical interactions and they produced more porosity than GP-MWCNTs due to surfactant remaining on MWCNTs surface. XRD confirmed the degree of C-S–H formation in the cement matrix rose with cure time. Both AP-MWCNTs and GP-MWCNTs showed similar rates of C-S–H formation from cement hydration, but the pore area inside the cement composites was significantly different. AP-MWCNTs exhibit higher electrical conductivity (8.27×10^{-4} S/cm vs. 5.86×10^{-4} S/cm) but a lower spreading coefficient compared to GP-MWCNTs. Consequently, AP-MWCNT/C showed higher electrical conductivity, while GP-MWCNT/C yielded higher mechanical strength, due to lower porosity inside the composites. The comparison of AP- and GP-modified MWCNTs highlights their potential for optimizing cement composite performance, focusing on the effect of the nanotube dispersion on increasing hydration reaction of cement and high mechanical strength and adding electricity in cement. Additionally, bifunctional MWCNTs with PIn—an electrically conductive polymer and PVAc—a hydrophilic polymer known for flexibility and low toxicity improved the dispersion of the MWCNTs in water during the cement hydration, reducing the pore in the cement. PIn functionalized on MWCNTs provides the electrically conductive property with its heteroaromatic structure for further capability to ECCCs application.

Acknowledgements
The authors wish to thank Thailand Science Research and Innovation (TSRI) and SCG Cement Co., Ltd., Thailand, for the "Research and Researchers for Industry (RRi) Fund", contract number PHD 62I0033, which provides for Miss Suthisa Onthong's Ph.D. study and her research. We would like to acknowledge the support from the Center of Eco-Materials and Cleaner Technology, Chemical Engineering Department and the Construction and Building Materials Research Center, Civil Engineering Department, KMUTNB, for lab equipment support and cement testing, respectively. We also wish to thank Research and Innovation, SCG Cement Co., Ltd., Thailand Center and Dr. Wilasinee Hanpongpunc for her help on the cement hydration testing and interpretation. Financial support was provided by the University of Oklahoma Libraries' Open Access Fund.

Author contributions
Suthisa Onthong: conceptualization, methodology, investigation, data and statistics analysis, writing–original draft, writing–review and editing. Wilasinee Hanpongpun: investigation, data analysis and interpretation, resources. Sakprayut Sinthupinyo: data interpretation, resources, funding acquisition. Edgar A. O'Rear: conceptualization, data analysis, writing–review and editing, supervision. Thirawudh Pongprayoon: conceptualization, data analysis, writing–review and editing, supervision, project administration.

Funding
The work was supported by National Research Council of Thailand (NRCT) contract number PHD 62I0033.

Availability of data and materials
The datasets used and/or analyzed during the current study are available from the corresponding author on reasonable request.

Declarations

Competing interests
The authors declare that they have no known competing financial interests or personal relationships that could have appeared to influence the work reported in this paper.

Received: 7 December 2024 Accepted: 3 June 2025
Published online: 25 August 2025

References

Aïtcin, P.-C. (2016). Portland cement. In Pierre-Claude Aïtcin & R. J. B. T.-S. and T. of C. A. Flatt (Eds). Woodhead Publishing. pp. 27–51. https://doi.org/10.1016/B978-0-08-100693-1.00003-5

AlMarzooqi, F. A., Bilad, M. R., Mansoor, B., & Arafat, H. A. (2016). A comparative study of image analysis and porometry techniques for characterization of porous membranes. *Journal of Materials Science, 51*, 2017–2032.

Amziane, S. (2006). Setting time determination of cementitious materials based on measurements of the hydraulic pressure variations. *Cement and Concrete Research, 36*(2), 295–304. https://doi.org/10.1016/j.cemconres.2005.06.013

Basheer, B. V., George, J. J., Siengchin, S., & Parameswaranpillai, J. (2020). Polymer grafted carbon nanotubes—Synthesis, properties, and applications: A review. *Nano-Structures and Nano-Objects, 22*, 100429. https://doi.org/10.1016/j.nanoso.2020.100429

Bullard, J. W., Jennings, H. M., Livingston, R. A., Nonat, A., Scherer, G. W., Schweitzer, J. S., et al. (2011). Mechanisms of cement hydration. *Cement and*

Concrete Research, 41(12), 1208–1223. https://doi.org/10.1016/j.cemconres.2010.09.011
Cerro-Prada, E., Pacheco-Torres, R., & Varela, F. (2021). Effect of multi-walled carbon nanotubes on strength and electrical properties of cement mortar. *Materials, 14*(1), 1–13. https://doi.org/10.3390/ma14010079
Chen, S., & Li, Y. (2024). Preparation and mechanical properties of carbon nanotube cement-based composite materials for construction. *International Journal of Microstructure and Materials Properties, 17*(4), 377–391.
Cheng, X., Tian, W., Gao, J., He, L., Zhang, J., & Wang, X. (2023). Effect of multi-walled carbon nanotube size on electrical properties of cement mortar composites. *Magazine of Concrete Research, 75*(12), 595–606. https://doi.org/10.1680/jmacr.22.00103
Copeland, L. E., Kantro, D. L., & Verbeck, G. J. (1960). *Chemistry of hydration of Portland cement*. Citeseer.
Cui, X., Han, B., Zheng, Q., Yu, X., Dong, S., Zhang, L., & Ou, J. (2017). Mechanical properties and reinforcing mechanisms of cementitious composites with different types of multiwalled carbon nanotubes. *Composites Part a: Applied Science and Manufacturing, 103*, 131–147. https://doi.org/10.1016/j.compositesa.2017.10.001
Ding, S., Wang, X., Qiu, L., Ni, Y., Dong, X., Cui, Y., et al. (2023). Self-sensing cementitious composites with hierarchical carbon fiber-carbon nanotube composite fillers for crack development monitoring of a maglev girder. *Small (Weinheim an der Bergstrasse, Germany), 19*(9), 2206258.
Ding, S., Xiang, Y., Ni, Y.-Q., Thakur, V. K., Wang, X., Han, B., & Ou, J. (2022). In-situ synthesizing carbon nanotubes on cement to develop self-sensing cementitious composites for smart high-speed rail infrastructures. *Nano Today, 43*, 101438.
Dong, W., Li, W., Tao, Z., & Wang, K. (2019). Piezoresistive properties of cement-based sensors: Review and perspective. *Construction and Building Materials, 203*, 146–163. https://doi.org/10.1016/j.conbuildmat.2019.01.081
Dowdy, S., Wearden, S., & Chilko, D. (2011). *Statistics for research*. John Wiley & Sons.
Genetti, Wb., Yuan, W. L., Grady, B. P., O'Rear, E. A., Lai, C. L., & Glatzhofer, D. T. (1998). Polymer matrix composites: Conductivity enhancement through polypyrrole coating of nickel flake. *Journal of Materials Science, 33*, 3085–3093.
Hamid, S. A. (1981). The crystal structure of the 11Å natural tobermorite Ca2 25 [Si3O7. 5 (OH) 1.5]· 1H2O. *Zeitschrift Für Kristallographie-Crystalline Materials, 154*(3–4), 189–198.
Han, B., Zhang, L., Sun, S., Yu, X., Dong, X., Wu, T., & Ou, J. (2015). Electrostatic self-assembled carbon nanotube/nano carbon black composite fillers reinforced cement-based materials with multifunctionality. *Composites Part a: Applied Science and Manufacturing, 79*, 103–115. https://doi.org/10.1016/j.compositesa.2015.09.016
Han, B., Zhang, L., Zeng, S., Dong, S., Yu, X., Yang, R., & Ou, J. (2017). Nano-core effect in nano-engineered cementitious composites. *Composites Part a: Applied Science and Manufacturing, 95*, 100–109.
Hanawalt, J. D., Rinn, H. W., & Frevel, L. K. (1938). Chemical analysis by X-ray diffraction. *Industrial & Engineering Chemistry Analytical Edition, 10*(9), 457–512.
Hanumansetty, S., O'Rear, E.A., & Resasco, D. E. (2015). Hydrophilic encapsulation of multi-walled carbon nanotubes using admicellar polymerization. *Colloids and Surfaces a: Physicochemical and Engineering Aspects, 474*, 1–8. https://doi.org/10.1016/j.colsurfa.2015.02.047
He, S., Chai, J., Yang, Y., Cao, J., Qin, Y., & Xu, Z. (2023). Effect of nano-reinforcing phase on the early hydration of cement paste: A review. *Construction and Building Materials, 367*, 130147. https://doi.org/10.1016/j.conbuildmat.2022.130147
Jing, X., & Wu, Y. (2011). Electrochemical studies on the performance of conductive overlay material in cathodic protection of reinforced concrete. *Construction and Building Materials, 25*(5), 2655–2662. https://doi.org/10.1016/j.conbuildmat.2010.12.015
Li, H., Wang, H., Liu, C., Huan, X., Dong, J., Li, W., et al. (2022). PGMA-grafted MWCNTs: Correlation between molecular weight of grafted PGMA and dispersion state of MWCNTs–PGMA in an epoxy matrix. *Journal of Materials Science, 57*(16), 7997–8015.
Liu, C., Gai, W., Pan, S., & Liu, Z. (2003). The exothermal behavior in the hydration process of calcium phosphate cement. *Biomaterials, 24*(18), 2995–3003. https://doi.org/10.1016/S0142-9612(03)00125-X
MacLeod, A. J. N., Collins, F. G., & Duan, W. (2021). Effects of carbon nanotubes on the early-age hydration kinetics of Portland cement using isothermal calorimetry. *Cement and Concrete Composites, 119*(February), 103994. https://doi.org/10.1016/j.cemconcomp.2021.103994
Marchon, D., & Flatt, R. J. (2016). Mechanisms of cement hydration. In Pierre-Claude Aïtcin & R. J. B. T.-S. and T. of C. A. Flatt (Eds). Woodhead Publishing. pp. 129–145. https://doi.org/10.1016/B978-0-08-100693-1.00008-4
Mendoza, O., Sierra, G., & Tobón, J. I. (2014). Effect of the reagglomeration process of multi-walled carbon nanotubes dispersions on the early activity of nanosilica in cement composites. *Construction and Building Materials, 54*, 550–557. https://doi.org/10.1016/j.conbuildmat.2013.12.084
Metaxa, Z. S., Boutsioukou, S., Amenta, M., Favvas, E. P., Kourkoulis, S. K., & Alexopoulos, N. D. (2022). Dispersion of multi-walled carbon nanotubes into white cement mortars: The effect of concentration and surfactants. *Nanomaterials*. https://doi.org/10.3390/nano12061031
Mohammed, A. G., Ozgur, G., & Sevkat, E. (2019). Electrical resistance heating for deicing and snow melting applications: Experimental study. *Cold Regions Science and Technology, 160*(February), 128–138. https://doi.org/10.1016/j.coldregions.2019.02.004
Neves Junior, A., Toledo Filho, R. D., De Moraes Rego Fairbairn, E., & Dweck, J. (2015). The effects of the early carbonation curing on the mechanical and porosity properties of high initial strength Portland cement pastes. *Construction and Building Materials, 77*, 448–454. https://doi.org/10.1016/j.conbuildmat.2014.12.072
O'Rear, E. A., Onthong, S., & Pongprayoon, T. (2023). Mechanical strength and conductivity of cementitious composites with multiwalled carbon nanotubes: To functionalize or not? *Nanomaterials, 14*(1), 80.
Onthong, S., Pongprayoon, T., & O'Rear, E. A. (2024). Sequential admicellar polymerization of polyindole and poly (vinyl Acetate) for increasing electrical conductivity and water dispersion of multiwalled carbon nanotubes. *ACS Applied Polymer Materials, 7*(1), 187–199.
Onthong, S., O'Rear, E.A., & Pongprayoon, T. (2022). Enhancement of electrically conductive network structure in cementitious composites by polymer hybrid-coated multiwalled carbon nanotube. *Materials and Structures*. https://doi.org/10.1617/s11527-022-02070-z
Onthong, S., O'Rear, E.A., & Pongprayoon, T. (2023). Composite nanoarchitectonics by interfacial bonding for conductivity and strength development of grafted multiwall carbon nanotube/cement. *Construction and Building Materials, 392*, 131940. https://doi.org/10.1016/j.conbuildmat.2023.131940
Páez-Pavón, A., García-Junceda, A., Galán-Salazar, A., Merodio-Perea, R. G., Sánchez del Río, J., & Lado-Touriño, I. (2022). Microstructure and electrical conductivity of cement paste reinforced with different types of carbon nanotubes. *Materials, 15*(22), 7976.
Pang, X., Sun, L., Sun, F., Zhang, G., Guo, S., & Bu, Y. (2021). Cement hydration kinetics study in the temperature range from 15 °C to 95 °C. *Cement and Concrete Research, 148*(June), 106552. https://doi.org/10.1016/j.cemconres.2021.106552
Preece, S. J., Billingham, J., & King, A. C. (2001). On the initial stages of cement hydration. *Journal of Engineering Mathematics, 40*, 43–58.
Qin, H., Ding, S., Ashour, A., Zheng, Q., & Han, B. (2024). Revolutionizing infrastructure: The evolving landscape of electricity-based multifunctional concrete from concept to practice. *Progress in Materials Science, 145*, 101310. https://doi.org/10.1016/j.pmatsci.2024.101310
Rauniyar, B. S., & Bhattarai, A. (2021). Study of conductivity, contact angle and surface free energy of anionic (SDS, AOT) and cationic (CTAB) surfactants in water and isopropanol mixture. *Journal of Molecular Liquids, 323*, 114604. https://doi.org/10.1016/j.molliq.2020.114604
Saghiri, M. A., Shabani, A., Asatourian, A., & Sheibani, N. (2017). Storage medium affects the surface porosity of dental cements. *Journal of Clinical and Diagnostic Research: JCDR, 11*(8), ZC116–ZC119. https://doi.org/10.7860/JCDR/2017/28657.10517
Scrivener, K., Ouzia, A., Juilland, P., & Mohamed, A. K. (2019). Advances in understanding cement hydration mechanisms. *Cement and Concrete Research, 124*, 105823.
Siahkouhi, M., Razaqpur, G., Hoult, N. A., Hajmohammadian Baghban, M., & Jing, G. (2021). Utilization of carbon nanotubes (CNTs) in concrete for structural health monitoring (SHM) purposes: A review. *Construction and Building Materials, 309*(August), 125137. https://doi.org/10.1016/j.conbuildmat.2021.125137
Ståhle, L., & Wold, S. (1989). Analysis of variance (ANOVA). *Chemometrics and Intelligent Laboratory Systems, 6*(4), 259–272. https://doi.org/10.1016/0169-7439(89)80095-4

Sun, G., Liang, R., Lu, Z., Zhang, J., & Li, Z. (2016). Mechanism of cement/carbon nanotube composites with enhanced mechanical properties achieved by interfacial strengthening. *Construction and Building Materials, 115*, 87–92. https://doi.org/10.1016/j.conbuildmat.2016.04.034

Sun, S., Han, B., Jiang, S., Yu, X., Wang, Y., Li, H., & Ou, J. (2017). Nano graphite platelets-enabled piezoresistive cementitious composites for structural health monitoring. *Construction and Building Materials, 136*, 314–328. https://doi.org/10.1016/j.conbuildmat.2017.01.006

Torabian Isfahani, F., Li, W., & Redaelli, E. (2016). Dispersion of multi-walled carbon nanotubes and its effects on the properties of cement composites. *Cement and Concrete Composites, 74*, 154–163. https://doi.org/10.1016/j.cemconcomp.2016.09.007

Vaičiukyniene, D., Vaitkevičius, V., Kantautas, A., & Sasnauskas, V. (2012). Utilization of by-product waste silica in concrete-based materials. *Materials Research, 15*(4), 561–567. https://doi.org/10.1590/S1516-14392012005000082

Vazquez, A., & Pique, T. M. (2016). 5 - Biotech admixtures for enhancing portland cement hydration. F. Pacheco-Torgal, V. Ivanov, N. Karak, & H. B. T.-B. and B. A. for E.-E. C. M. Jonkers (Eds). Woodhead Publishing (pp. 81–98). https://doi.org/10.1016/B978-0-08-100214-8.00005-1

Vinod, A., Vijay, R., Manoharan, S., Vinod, A., Lenin Singaravelu, D., Sanjay, M. R., & Siengchin, S. (2019). Characterization of raw and benzoyl chloride treated Ipomoea pes-caprae fibers and its epoxy composites. *Materials Research Express, 6*(9), 95307. https://doi.org/10.1088/2053-1591/ab2de2

Wahid, Z., Latiff, A. I., & Ahmad, K. (2018). Application of one-way ANOVA in completely randomized experiments. *Journal of Physics: Conference Series*. https://doi.org/10.1088/1742-6596/949/1/012017

Wang, L., & Aslani, F. (2019). A review on material design, performance, and practical application of electrically conductive cementitious composites. *Construction and Building Materials, 229*, 116892. https://doi.org/10.1016/j.conbuildmat.2019.116892

Wang, X., Dong, S., Ashour, A., Zhang, W., & Han, B. (2020). Effect and mechanisms of nanomaterials on interface between aggregates and cement mortars. *Construction and Building Materials, 240*, 117942. https://doi.org/10.1016/j.conbuildmat.2019.117942

Wang, X., Feng, D., Shi, X., & Zhong, J. (2022a). Carbon nanotubes do not provide strong seeding effect for the nucleation of C3S hydration. *Materials and Structures, 55*(7), 172.

Wang, X., Dong, S., Li, Z., Han, B., & Ou, J. (2022b). Nanomechanical characteristics of interfacial transition zone in nano-engineered concrete. *Engineering, 17*, 99–109. https://doi.org/10.1016/j.eng.2020.08.025

Yuenyongsuwan, J., Sinthupinyo, S., O'Rear, E. A., & Pongprayoon, T. (2019). Hydration accelerator and photocatalyst of nanotitanium dioxide synthesized via surfactant-assisted method in cement mortar. *Cement and Concrete Composites, 96*, 182–193. https://doi.org/10.1016/j.cemconcomp.2018.11.024

Zhang, H., Cao, S., & Yilmaz, E. (2023). Carbon nanotube reinforced cementitious tailings composites: Links to mechanical and microstructural characteristics. *Construction and Building Materials, 365*, 130123. https://doi.org/10.1016/j.conbuildmat.2022.130123

Zhang, J., Xu, L., & Zhao, Q. (2017). Investigation of carbon fillers modified electrically conductive concrete as grounding electrodes for transmission towers: Computational model and case study. *Construction and Building Materials, 145*, 347–353. https://doi.org/10.1016/j.conbuildmat.2017.03.223

Zhao, L., Guo, X., Liu, Y., Zhao, Y., Chen, Z., Zhang, Y., et al. (2018). Hydration kinetics, pore structure, 3D network calcium silicate hydrate, and mechanical behavior of graphene oxide reinforced cement composites. *Construction and Building Materials, 190*, 150–163. https://doi.org/10.1016/j.conbuildmat.2018.09.105

Publisher's Note

Suthisa Onthong She graduated PhD in 2024 from the Department of Chemical Engineering, Faculty of Engineering, King Mongkut's University of Technology North Bangkok, Thailand. Additionally, she earned the experience for her partial PhD research in the School of Sustainable Chemical, Biological and Materials Engineering, University of Oklahoma, Norman, OK, USA. Currently she is a postdoctoral researcher at Polymer Colloids Lab, Department of Chemistry, Faculty of Science and Technology, Rajamangala University of Technology Thanyaburi (RMUTT), Thailand.

Wilasinee Hanpongpun She is a researcher (PhD) at SCG Cement Co., Ltd., Thailand.

Sakprayut Sinthupinyo He is a researcher (PhD), serving as the head of research at SCG Cement Co., Ltd., Thailand.

Edgar A. O'Rear He is a Professor (PhD) at School of Sustainable Chemical, Biological and Materials Engineering, University of Oklahoma, Norman, OK, USA.

Thirawudh Pongprayoon He is an Associate Professor (PhD) in the Department of Chemical Engineering, Faculty of Engineering, King Mongkut's University of Technology North Bangkok, Thailand.